

## The Impacts of Human Activities on the Hydrogeological Regime of East Nile Delta, Egypt

Basma M. H. Mansour, Ahmed E. El-Rayes\* and Mona F. Kaiser

Geology Department, Faculty of Science, Suez Canal University, Ismailia, 41522, Egypt



### ABSTRACT

Human activities contribute numerous hydrogeological threats including waterlogging, soil salinization and water pollution in East Nile Delta region. Landsat Thematic Images were utilized to detect the environmental changes in the study area during the last three decades. Remote sensing and Geographic Information Systems data were integrated to monitor and measure surface areas of agricultural and urban developments. Risk assessment maps were constructed for waterlogging and soil salinization threats. The results cleared that both evaporation from logged and flood irrigation water surfaces cause up to 30% of water loss. The logged areas increased from 25km<sup>2</sup> in 1984 to 180km<sup>2</sup> in 2014 along the El-Tina plain which represents the most threatened zone. The total changes of waterlogging cover at east Nile Delta varies between 930km<sup>2</sup> in 1989, 685km<sup>2</sup> in 1998 after the construction of El-Salam Canal and 1044km<sup>2</sup> in 2014. The total estimated water loss by direct evaporation was up to 23.6Mm<sup>3</sup>/year. Following the construction of El-Salam Canal in 1998, water and drainage effluents into Manzala Lake were decreased creating shrinkage in its surface area by 45%. Consequently, water quality of Manzala Lake was severely deteriorated due to the throwing of municipal and irrigational sewages.

**Keywords:** Nile Delta, Human impacts, Waterlogging, Soil salinization, Risk assessment, Problem Management.

### INTRODUCTION

#### Location

The study area covers the eastern portion of the Nile Delta constituting a major part of flood plain lying between longitudes, 31° 30' - 32° 30'E and latitudes 30° 30' - 31° 30'N (Fig. 1). It is bounded to the north by the Mediterranean Sea, to the south by desert rolling plains and foot hills of Tertiary and Cretaceous structural ridges varying in altitudes between 200-800masl. To the northwest, it is bounded by Damietta Nile Branch while, the International Suez Canal Route represents its nowadays eastern boundary (it was the Isthmus basin

before the canal digging in 1869, -20masl). The Eastern Nile Delta Flank constitutes about 1% (about 10,000km<sup>2</sup>) of the Egyptian lands that is totally covered by Quaternary deposits of silt, clay and sands with thickness varying between 200m at the south and 700m at the north.

The flood plain fans out by gentle slopes of an order of 0.3m/km and then plains of very low gradient to the north through a distance of about 160km. Manzala Lake and its surroundings, characterize wet low lands connected via narrow brag with the Mediterranean Sea (Fig 1).

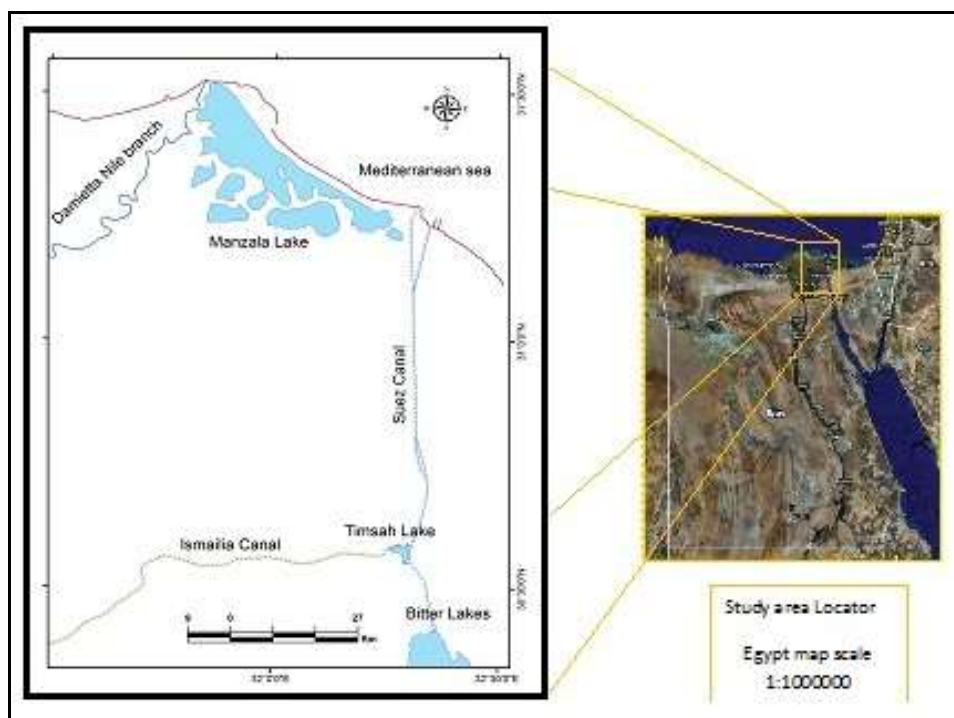


Figure (1): Location map of Eastern Nile Delta area.

### Problem Definition

The eastern Nile Delta of Egypt is a very promising area for development since it has a prominent watershed having abundant water resources. Unfortunately, it is suffering from rapid environmental degradation including: natural factors; such as land subsidence, rising of the sea level as a result of climatic changes (global warming) as well as anthropogenic factors; such as haphazard irrigation, mis-landuse and damming. These factors were increased especially after the closure of Aswan Dam in 1964, which reduced the agriculture productivity and altered the chemistry of Delta lagoon and lake waters (Klemas and Abdel Kader, 1982).

The Aswan Dam now controls the flood cycle, which previously flushed the delta plain and trapped the sediments at Lake Nasser behind it, reducing the nutrients previously carried downstream to the Delta

and contributing to the acceleration of coastal erosion by Mediterranean near shore currents. Many new agricultural projects were carried out in east Nile Delta area, while after few years of starting these projects, several surface water ponds were created followed by soil salinization resulted by evaporation of the logged water (Fig.2).

Many lands, including the underground infrastructure and irrigation nets, farmer houses, electricity towers, and even the administration buildings of the project managers, were drowned under the logged water. Subsequently there are risky levels of water pollution and land degradation leading to the loss of fertile soil and large amount of water without any beneficial usage. Human activities also involve pollution of several natural lakes such as: Manzala Lake due to dumping of industrial and agricultural sewages.



Figure (2): Different forms of land degradation in Eastern Nile Delta area (soil salinization and waterlogging).

### Objectives

The present study aims to assess, manage and protect the water resources quality and potentiality of the Eastern Nile Delta area, follow up the human activities within the area and their geo-environmental impact on formulating the groundwater flow regime and soil salinization along the Eastern flank of the Nile Delta, observe the groundwater flow directions and

chemical changes at the study area and its surrounding and predict the most susceptible sites for produced hazards using Groundwater Modeling and Geographic Information System.

### MATERIALS AND METHODS

The methodological approach is built on the basis of following the present hydrogeological status of the area;

This could be accessed through different ways which include:

- a) Collecting and conducting hydrochemical analyses on water samples from existing wells and water bodies for a number of 57 samples. Trace metals (20 samples) and bacterial analyses (12 samples) were conducted on groundwater from the study area.
- b) Measuring the groundwater levels and monitoring their seasonal variations during the winter seasons for years 1992, 2003 and 2013.
- c) Drawing the hydrogeologic cross section to define the water bearing formations.
- d) Monitoring land cover changes using Thematic Mapper (TM) images 4 & 5 (1989, 1998) and Operational Land Imager (OLI) image 8 (2014) that were picked in the winter seasons (Table, 1). The detected land cover changes include vegetation, surface water and bords, salt crust, un-used lands and urban areas and applying change detection technique for this purpose.

Water samples were collected during the field survey in July, 2013. Field measurements and laboratory analysis provided information on the depth to water, total depth of the well, subsurface lithology, physical and chemical properties of water and water quality. All these information were used to predict the recharge history of the groundwater in the study area. The samples were collected from different sources such as Nile River, Mediterranean Sea, Shallow and deep groundwater wells. The physical parameters of the collected water samples including specific conductance, pH-value and temperature were measured electrometrically in the field while, chemical analyses of the collected water samples were carried out at the hydrogeological laboratory of Geology Dept., Suez Canal University for determining the major ion constituents and total dissolved solids according to APHA, (1971), while a number of 20 samples were analyzed in Tuebingen University, Germany for trace metal analyses.

**Table (1):** Multispectral bands of Landsat 5 and Landsat 8 satellite images.

	<b>Landsat 4, 5 (1989, 1998)</b>	<b>Landsat 8 (2014)</b>
<b>Scanning system</b>	Thematic Mapper (TM)	Operational Land Imager (OLI) & Thermal Infrared Sensor (TIRS)
<b>Operating</b>	Since 1982	Since 2013
<b>Pixel size</b>	30×30m	30×30m
<b>Spectral</b>	Band 1 0.45 to 0.52 microns Blue-Green Band 2 0.52 to 0.60 microns Green Band 3 0.63 to 0.69 microns Red Band 4 0.76 to 0.90 microns NIR Band 5 1.55 to 1.75 microns MIR Band 7 2.08 to 2.35 microns MIR	Band 1 0.433 to 0.453 microns coastal & aerosol Band 2 0.450 to 0.515 microns Blue Band 3 0.525 to 0.600 microns Green Band 4 0.630 to 0.680 microns Red Band 5 0.845 to 0.885 microns NIR Band 6 1.560 to 1.660 microns MIR Band 7 2.100 to 2.300 microns MIR Band 9 1.360 to 1.390 microns Cirrus
<b>Thermal Channel</b>	Band 6 10.4 to 12.5 microns (120×120m)	Band 10 10.30 to 11.30 microns Band 11 11.50 to 12.50 microns (100×100 m)
<b>Panchromatic Channel</b>	Band 8 0.500 to 0.680 microns (15×15m)	Band 8 0.500 to 0.680 microns (15×15m)

## RESULTS AND DISCUSSION

### Hydrogeologic Setting

The Eastern Nile Delta is characterized by arid climate with hot and rainless summer, and mild winter with scarce rainfall (30-100 mm). These desert conditions left very little doubt that precipitation has any recharge effect on the present groundwater recharge flux. Physiographically, the Eastern Nile Delta is consists of two deltaic plains; the young deltaic plain comprises the main portion of the fertile and cultivated lands; and the old deltaic plain that stretches to the east and south of the modern flood plain. The old plain is consisting of gravely sand sheets of considerable thicknesses varying between 50m along the northern sector to 200m along the northern one. It is surrounded by structural ridges of Tertiary rocks on their south and south-eastern borders.

From these ridges, the gravely sand sheets slope by an order of 4m/km and then plains of very low gradient to the north. Some depressions are encountered such as, Wadi El-Ashra and Wadi El-Tumilat to the south and Manzala Lake and sabkhas to the north (Fig. 3).

Water-bearing formations of east Nile delta consist mainly of Quaternary fluvial and local fluvio-marine sand deposits. Their lithologic characteristics and thickness are highly controlled by the prevailing geological and environmental conditions. There are two types of water-bearing formations; the main fluvial Pleistocene aquifer and the local fluvio-marine Holocene semi-permeable aquifer. The Quaternary sediment is underlined by Miocene and Pliocene successions of limestone and shale respectively, which act as an impervious base for the main Quaternary aquifer in most areas (Fig. 4). The Pliocene shale,

according to Geriesh (1995), shows foreshore to relatively deep quiet marine character deposited under transgressive sea, whereas the Quaternary, sandstones at the top seem to have been deposited under rather regressive sea. The global glacial-eustatic variation in the sea level was the most effective paleo-environmental conditions on the Nile delta Formation,

especially during the Quaternary period (Shata and El Fayomy, 1970 and Zaghloul, et al., 1979). Nowadays, waterlogging and soil salinization are the most prevailing desertification phenomena (Fig. 2) that greatly affect the degradation of the fertile soil and losing a huge amount of Nile water at the northern coastal zone.

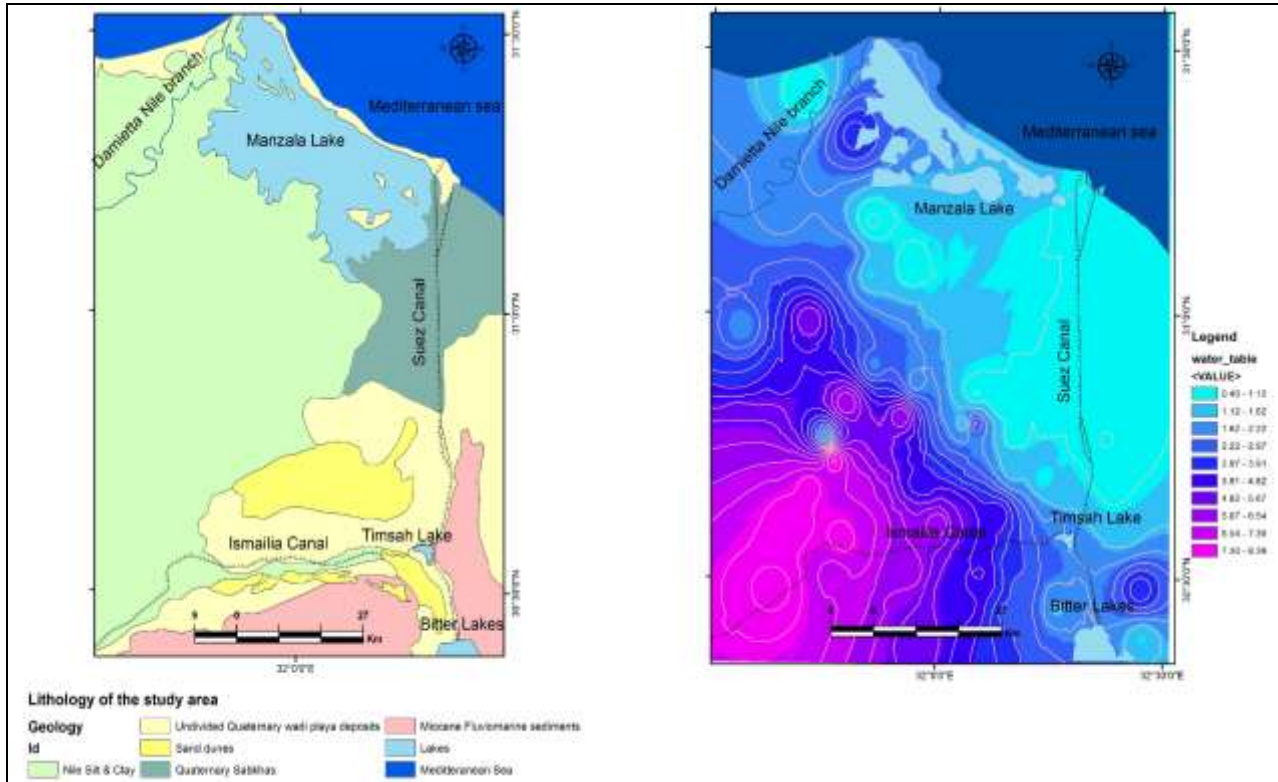


Figure (3): Geologic map (left), groundwater table map (right) of the Eastern Nile Delta area.

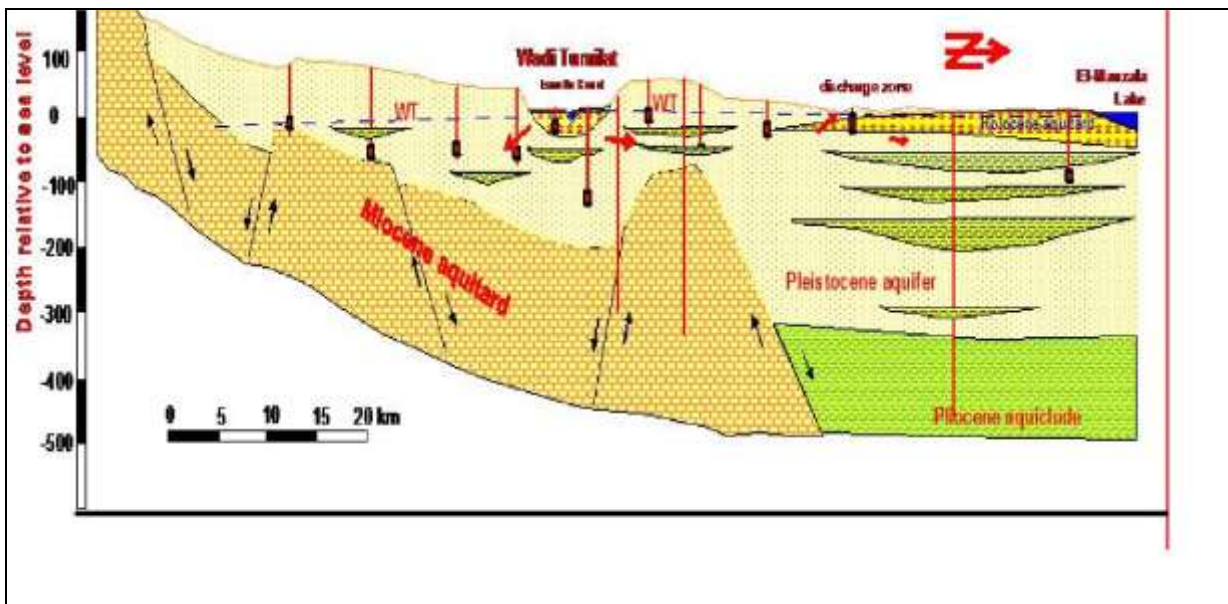


Figure (4): Hydrogeological cross section from South to North along the Eastern Nile Delta area (after Geriesh, 1989-See Fig. 3 for location).

Groundwater recharge to the Quaternary aquifers could take place through both the seepage from canal water distributaries and the excess irrigation return flow in the traditionally cultivated lands all over the study area and the newly reclaimed desert fringes to the east (Fig. 3 and 4). Rainstorms may also contribute to a little recharge especially on the northern sand dunes and beach sediments due to the relative high rainfall rate (70–100 mm/year) but we can't believe it as a source of recharge for the deeper aquifers along the delta apex and the dry desert fringes where it doesn't exceeds 30 mm/year. Sewage effluent from several hundreds of Villages constitutes additional source for shallow groundwater recharge due the absence of sewage disposal

sal system in most of these villages.

### Groundwater Geochemistry

#### *Salinity distribution*

The carried out hydrochemical analyses (Table 2) indicate that salinity of the examined water has wide variability and ranges in Pleistocene aquifer between 478 – 10,340 mg/l (Fig. 5). The lowest concentration is observed in W13 at the southern flood plain and the highest one is observed in W45 along the eastern coastal plain, east of Suez Canal Navigation Rout. While in the Holocene aquifer, it varies between 532- 25500 mg/l in E3 at the western Nile Delta flank and in E26 along the middle coastal zone respectively.

**Table (2):** General Indication of Pollution Threats by Different Chemical and Microbiological Constituents in Relationship to the EPA\* and EHCW Standards.

Parameters	EPA Standard	EHCW Standard	Analyzed samples		
			No. of samples	Range min-max	Average
<b>Physical and major</b>					
PH	6.5-8.5	6.5-9.2	57	7.1-8.2	9.98
TDS mg/L	500	1200	57	478-25500	<b>5643</b>
SAR	0-9*	No index	57	2.7-13.5	5.8
TH (mg/L as CaCo3)	100	500	57	<b>60-1265</b>	<b>560</b>
Calcium mg/L	75	200	57	20-890	200
Magnesium mg/L	30	150	57	4.8-780	133
Sodium mg/L	No index	200	57	74-7487	<b>1614</b>
Potassium mg/L	No index	No index	57	2-22	7.4
Hydrocarbonate mg/L	No index	No index	57	116-586	295
Sulfate mg/L	200	400	57	14.7-4116	<b>733</b>
Chloride mg/L	200	500	57	<b>39-11786</b>	<b>2123</b>
<b>Trace and Toxic</b>					
N-Nitrate mg/L	10	10**	57	1.8- <b>32</b>	5.8
Phosphate mg/L	1	No index	57	<b>0.5-3.1</b>	<b>1.1</b>
Iron mg/L	0.3	0.3	20	0.004-0.17	0.085
Cadmium mg/L	0.01	0.005	20	<b>0.002-0.12</b>	<b>0.008</b>
Lead mg/L	0.05	0.05	20	0.001-.008	0.003
Strontium, mg/l	No index	4.0	20	0.21-9.25	2.78
Zinc mg/l	0.05	0.05	20	0.002-0.03	0.007
<b>Microbiological content colony/100ml</b>					
Total bacterial count	0.0	0.0	12	<b>0-11,000</b>	<b>1,050</b>
Fecal Coliform/ml	0.0	0.0	12	<b>0-400</b>	<b>128</b>

The distribution of total dissolved solids of all the obtained hydrochemical results of the examined samples shows irregular changes along the southwest - northeast trend (Figs. 5). From this map, the following can be obtained;

a) Salinity distribution of groundwater has a wide range and gradually increases from fresh water type, in both shallow Holocene and deep Pleistocene aquifers along the southern Nile Delta apex, to highly saline water along the northern and eastern coastal zones facing the Mediterranean and Suez Canal Navigation Route respectively. However, the shallow aquifer shows a significant increase in salinity than the deeper aquifer.

High salinity values are most probably due to the leaching of salt content in sediments of these low laying coastal zones which has fluvio-marine characters along the northern and eastern low lands.

b) The water table along northern coastal areas is remarkably high and forms a water mound (Fig. 6). There is a conformable relation with the groundwater flow regime of the study area which is also concordant with our hypothesis that considers the rule of evaporation in increasing water salinity of the groundwater at the study area.

The salinity extended outwards the discharging zone south of Manzala Lake; could be attributed to the effect

of evaporation (Salt crusts and bands of gypsum and calcite are observed on the soil surface of these areas). The deep groundwater well (W28) north of this zone, just close to the Lake has fresher water composition and lower salinity (1720mg/l) than the shallow groundwater at this zone.

It is worth to mentioning here that the salt contents of Manzala Lake water along the coastal zone is very low compared with the seawater. It varies between 1600-10650 mg/l from its entrance to the outlet barrage. This difference could be attributed to the large aerial

extension of Manzala Lake and the effect of evaporation under high fresh water recharge. The main ion-dominance distribution is;  $Na > Ca > Mg$  and  $Cl > SO_4 > HCO_3$ . The order of cations concentration changes to be  $Na > Mg > Ca$  in the northern low lands and  $Ca > Na > Mg$  in the southern part of the Nile Delta. The order of anions is changed to be of  $HCO_3 > Cl > SO_4$  dominant order along the southern part of the Nile Delta and the western reaches of Wadi El Tumilat. Also, the order is changed to  $SO_4 > Cl > HCO_3$  in some localities along the eastern low lands.

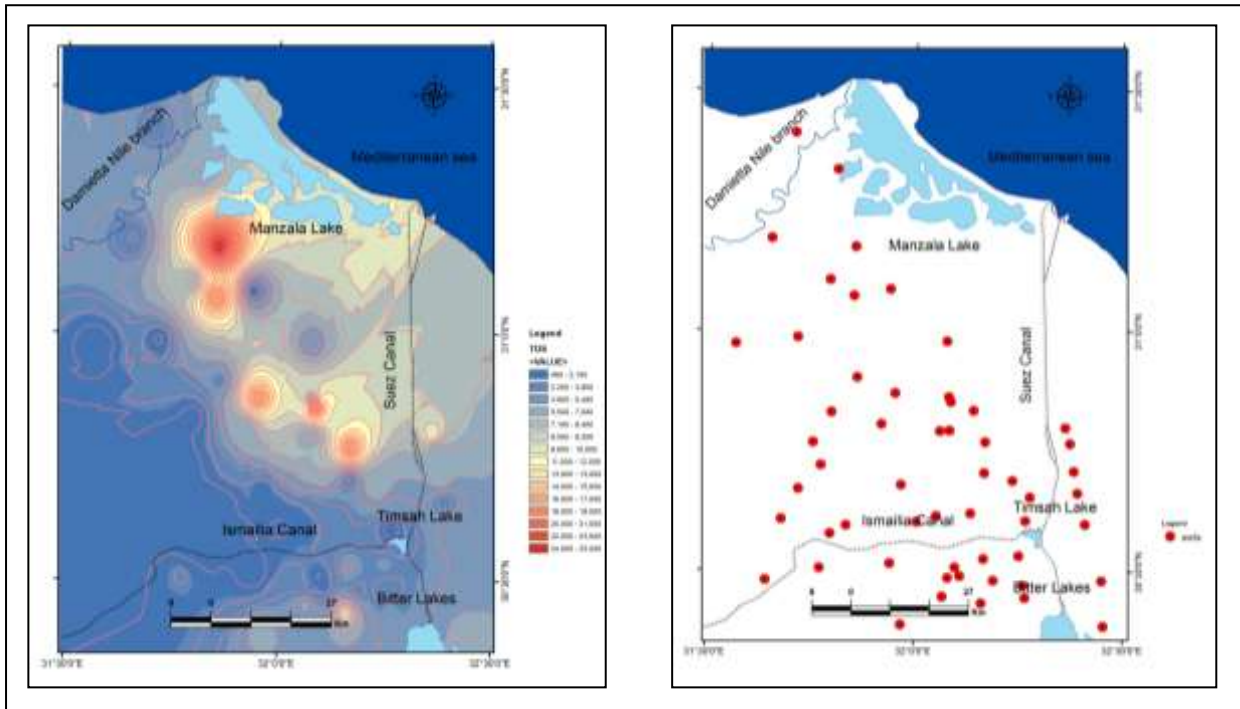


Figure (5): Well Location map of the eastern Nile Delta area to the right and TDS (in mg/l) distribution map to the left.

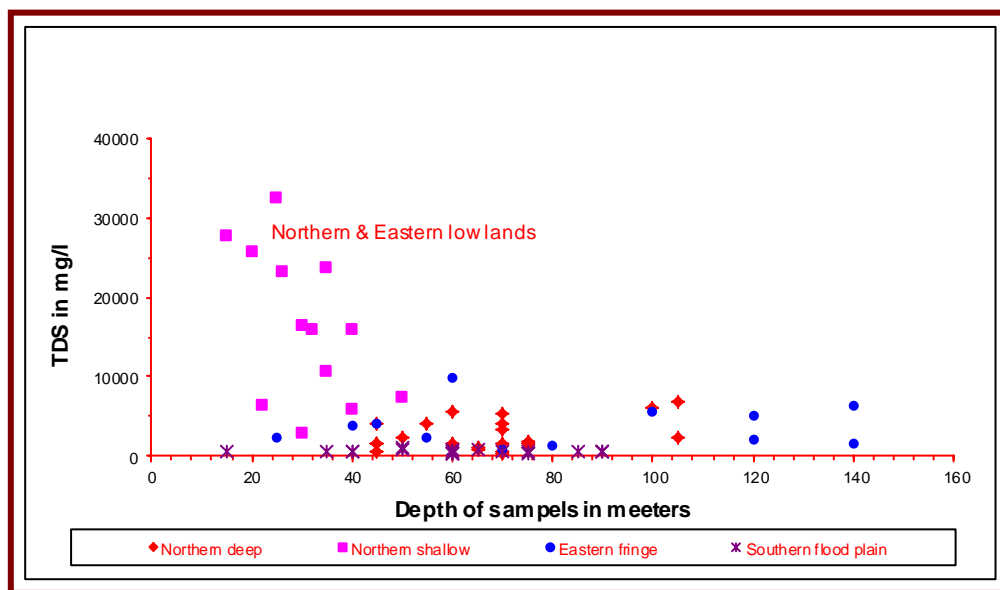


Figure (6): Relationship between TDS and depth of groundwater.

Generally we can attribute this gradual change to a previously invaded sea especially during the Holocene time (Holocene transgression) where, the northern water samples are near to the seawater in its composition, while the composition of the southern water is more close to the Nile water composition.

A sudden decrease in the total dissolved salt content with depth of water samples, along the northern low lands close to the coastal lakes, has been observed between the upper saline aquitard and the lower main aquifer (Table 2 & Fig. 5). This decrease is very low in the areas of the eastern flank of the delta. In the eastern low lands, salt content decreases gradually with depth along their contact with the underlying main aquifer (Fig. 6, which may prove that, the hydraulic connections between these two aquifers along these low land areas are a prevailing case.

*Hydrochemical facies*

The constructed hydrochemical facies map (Fig. 7) shows that, the groundwater resources in the study area are represented by six hydrochemical facies. These facies are; Ca-HCO<sub>3</sub><sup>-</sup>; Na<sup>+</sup>-HCO<sub>3</sub><sup>-</sup>; Na<sup>+</sup>-Mix (no dominant anion), Na<sup>+</sup>-Cl<sup>-</sup> (Na surpluses); Na<sup>+</sup>-Cl<sup>-</sup> (Na<sup>+</sup>

deficit) of old marine origin (Ca>Mg) and Na<sup>+</sup>-Cl<sup>-</sup> of recent marine origin or interference (Mg>Ca). These facies are distributed as a well-developed zonation form around the Nile distributary, Damietta branch, Wadi El-Tumilat and Pelluesic Nile branch, especially their upstream reaches. This well-developed zonation form started by Ca<sup>++</sup>-HCO<sub>3</sub><sup>-</sup>, Na<sup>+</sup>-HCO<sub>3</sub><sup>-</sup>, Na-mix fresh water type and ended by Na<sup>+</sup>-Cl<sup>-</sup> brackish to saline water type from the southern delta apex towards the northern and eastern directions respectively. This gradual changes of the hydrochemical facies from south west to north east can be attributed to a mixing process between two main water types; the first is characterized by Na HCO<sub>3</sub> - Na-mix fresh water composition and represents the southern delta apex and the most proximities of the Nile distributaries system while, the second is characterized by Na-Cl- composition and represents the northern and north-eastern parts of the old Holocene shore line proximities. There is another but low dominant third water type of Na-Cl- type (Ca>Mg) characterized the most south eastern parts along the desert fringes of the delta. The intermediate zones are characterized by transitional composition between these mentioned types.

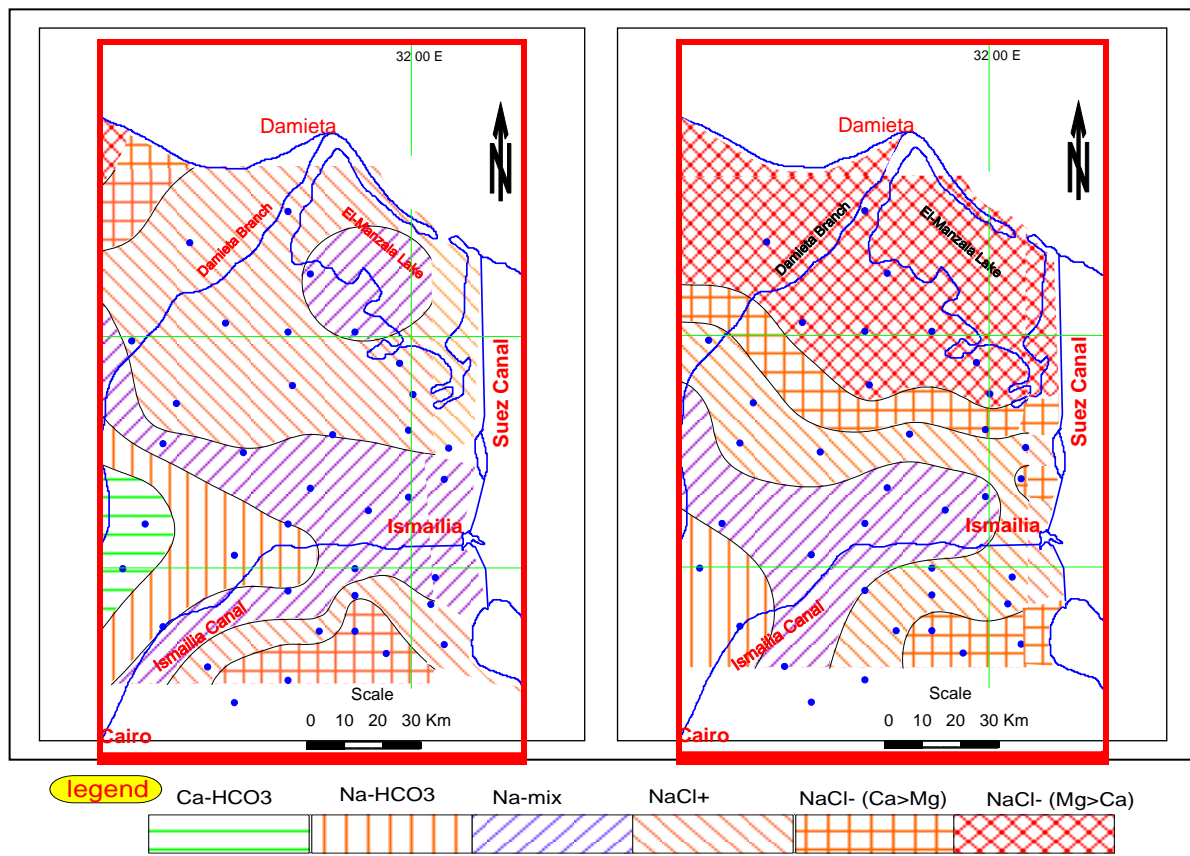


**Figure (7):** Distribution of the groundwater hydrochemical facies in the Pleistocene (A) and the Holocene (B) aquifers along the eastern Nile Delta Region.

Na/Cl ratios in the transitional water types are higher than that of the seawater (Table 1). In some localities along the eastern side of the Nile Delta, Ca and SO<sub>4</sub> exceed Mg and Cl proportions respectively. Also, HCO<sub>3</sub> ion present in a higher concentration than that recorded in the southern parts of the delta. Na is the most predominance ion and reaches up to 90 %.

According to the previously mentioned observations, the following hydrochemical facies are identified:

- i. Ca (HCO<sub>3</sub>)<sub>2</sub> and Na HCO<sub>3</sub> types represent the southern part of the Nile Delta.
- ii. Na HCO<sub>3</sub> and Na-mix (no dominance anion) types represent the middle parts of the study area and the western part of Wadi El Tumilat and old Pelluesic Nile branch, as well as, its surrounding parts to all directions.
- iii. Na Cl (Na surplus type) represents the eastern low lands and the outer zone of the second water type - area.
- iv. Na Cl (Na deficit type) represents the northern low lands along the coastal shore line and with Mg > Ca, and the southern reaches of the desert fringes to the southeast but with Ca > Mg.

The Na-mix type refers to water in which no single anion makes up more than 50 % of the sum of all anions. It is expected to be a transitional water type

between Na HCO<sub>3</sub> and Na Cl water composition. Na enrichment occurred during flushing especially in the fine and loamy sand soils.

### Pollution and Hazard Indicators

#### Nutrients

The results indicated that the nutrients; nitrates and phosphates (Table 2) exist in high proportions in and around the village reaches of the coastal area and Wadi El-Tumilat depression. Nitrate is found in critical values in most of the investigated samples and it is well correlated with the increase of sulphate along the same areas (Fig. 8) which could be used as indicator for human impacts. Their concentration levels are much higher in most cases than the recommended safe limits proposed by EHCW (1995) for drinking water. Therefore, it is recommended to monitor this water periodically. The high Nitrate concentration in drinking water affects negatively the body development and nervous and heart systems, especially for children. It causes also methemoglobinemia (blue baby disease) for the infants (Bouwer, 1978). It is worth to mentioning here that, using this contaminated water in fish farming could produce a serious health problem.

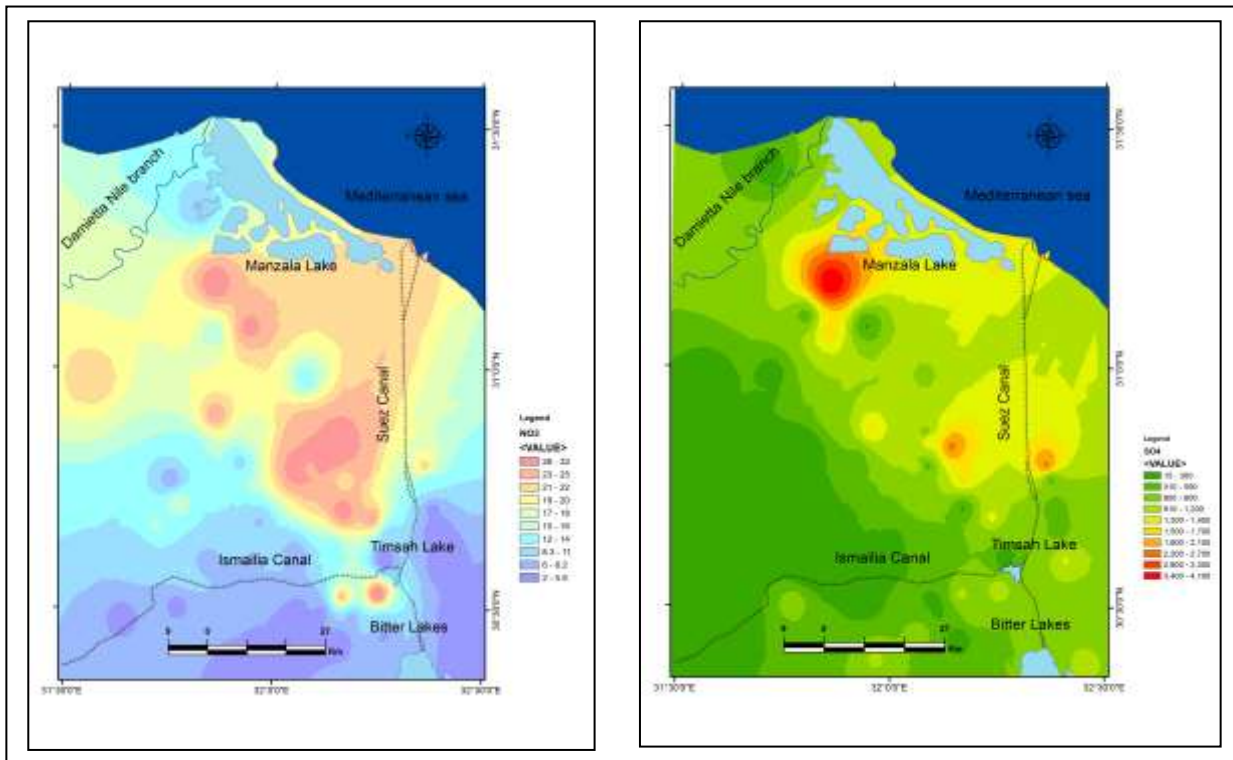


Figure (8): Nitrate (left) and Sulphate (right) distribution maps in groundwater of eastern Nile Delta area (Values in mg/l).

#### Trace metals

The trace elements: Pb, Cd, Fe, Sr and Zn are obviously the elements of greatest concern for water quality assessments for drinking and irrigation purposes. Results of these analyses (Table 2) indicated that a considerable number of the

examined samples have concentrations higher than the maximum permissible standard for drinking water that recommended by the EPA (1975) and the Egyptian Higher Committee of Water - EHCW (1995). This critical increase is detected mainly in the northern and eastern low lands (Fig. 9). This could be attributed

to the urbanization and agricultural activities along these areas. High Cd and Pb contents in drinking water are very dangerous because they have poisoning effect. Their concentrations exceed the optimal drinking water

level in most of the examined samples (especially Cd). High Cd causes high blood pressure, and kidney damage. While, high Pb level causes kidney disease and disturbances in the central nervous system.

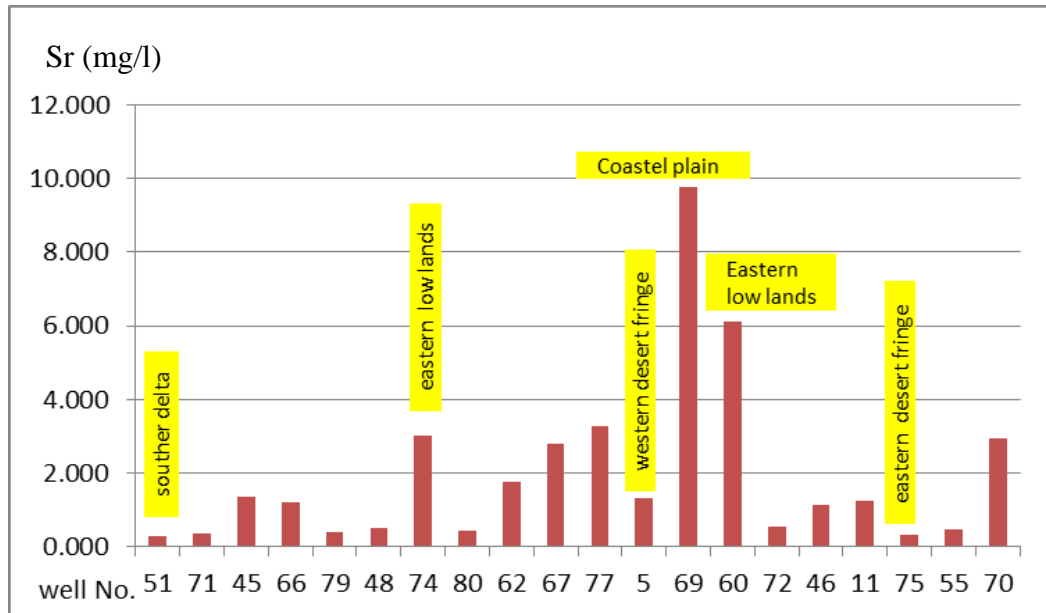


**Figure (9):** Distribution of Sr in the examined groundwater of the eastern Nile Delta area.

### Remote Sensing and Change Detection

Supervised classification (Fig. 10) was completed for each date using field observations collected from more than 34 ground checkpoints and digital topographic maps of the study area. Extraction of the five geomorphologic classes from 1989 to 1998 and 1998-2014 images was assisted by image classification. El-Salam Canal Development Projects were responsible for both the shrinking of Manzala Lake and the increase waterlogging and urban land use surface area in 1998 and 2014 after the completion of canal digging process. Most of the drain water that was effluent to Manzala Lake has been reduced from 7.5 billion m<sup>3</sup>/y to 3.5 billion m<sup>3</sup>/y after the canal digging in 1998. The surface area of cultivated land also increased from 3620 km<sup>2</sup> in 1989 to 3760 km<sup>2</sup> in 2014 (Fig. 10) due to land reclamation processes.

Waterlogging and wetland areas (red in the figure) and sabkhas and salt crust surfaces (green) were also increased from 930 km<sup>2</sup> and 360 km<sup>2</sup> in 1989 to 1044 km<sup>2</sup> and 1356 km<sup>2</sup> in 2014 respectively. This increase in wetland habitats is caused primarily by human activities including the creation of fish farms; groundwater level rises and water return flow from the irrigation practices. This increase of land covers surface area along the coastal areas could be attributed to various processes such as sea level rise, land subsidence and low topographic relief. In order to verify and validate the primary results of the satellite image classification, field surveys were conducted at specific sites. Image data obtained through remote sensing were integrated with

data collected from topographic and morphologic maps and field investigations in order quantify the environmental changes on the study area during 1984–2000 and 2010. The impact of El-Salam Canal on waterlogging was very remarkable. The observed land use/land cover changes were caused by several factors (Arnous and Green, 2015). The study area has been subjected to intensive local planning and development projects such as construction of the El-Salam Canal, the creation of the East Port Said harbour, an increase in industrialization, fish farms and reclamation. From 1926 to 1987, the sea level rose 16 cm (average rate of 2.6 mm/year) and it is likely that sea level will continue to rise by another 44.2 cm by 2100 (Frihy, 1992).

### Problem Management

The control of waterlogging can be achieved using appropriate drainage system to prevent water discharge at the surface soil and cease soil salinization. The removal of the stored salts in the soil root zone would take consequent tens to hundreds of years, even under good enhanced flushing rates. Some farmers tried to overcome the waterlogging problem either by converting their farm lands to fish farms or sand fills their wet lands which seems to be useless in solving this problem.

The most realistic way to prevent waterlogging and soil salinization is to manage the cause and cut off the supply of water producing excess groundwater recharge across agricultural landscape. Occasionally, groundwater is collected via open ditches to avoid

waterlogging problem. However, such ditches take land out of production and require considerable cleaning and other maintenance. Instead, subsurface drains (Fig. 11) and dewatering wells are wildly used to lower water level in the logged areas. In this study we discuss the

waterlogging risks, hazards and causes as revealed from the integrated hydrogeologic and remote sensing investigations. Upon these results, we simulate the problem and recommend some designs to solve and remediate its hazards.

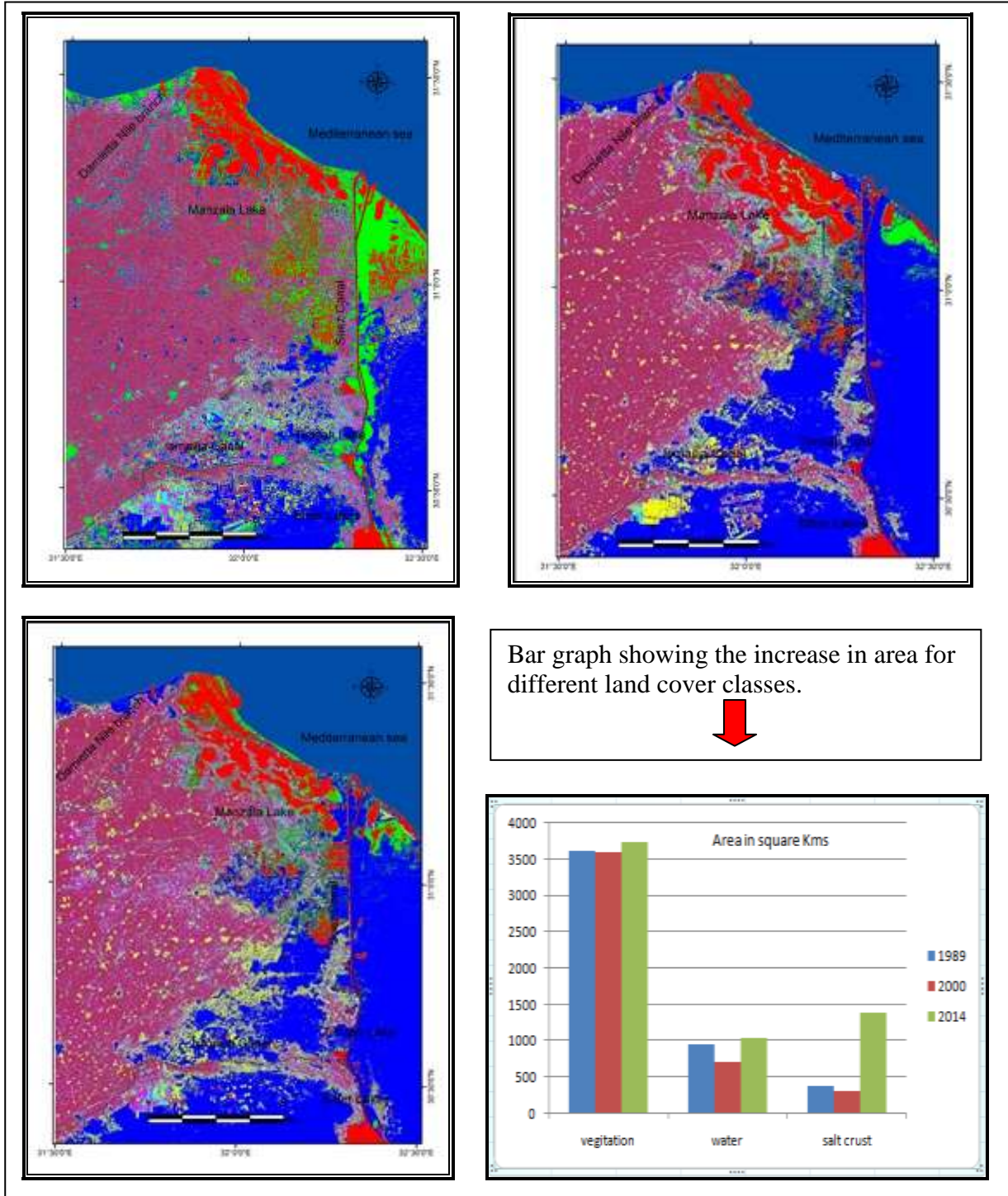


**Figure (10):** Monitoring land cover changes using landsat images 5 (1989, 1998) and 8 OLI (2014) that were picked in the winter season. for Land change detection during the period from; 1989 (lower left); 1998 (upper right) and 2014 (upper left). The wetlands (red), salt crust (pale green) and vegetation cover (Violet) are shown.

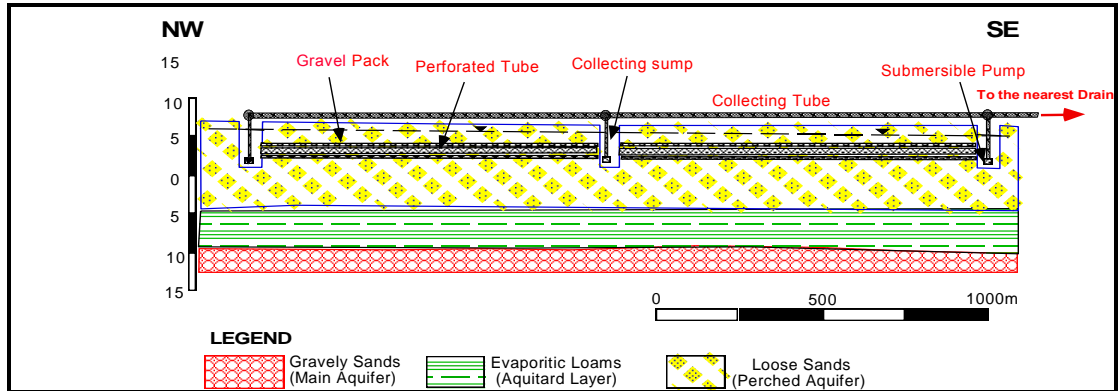


**Figure (11):** Proposed subsurface drain design for improving drainage efficiency of the logged water sites.

The present study proposes two solution models for improving drainage efficiency using underground subsurface drains along the eastern sector to prevent saltwater intrusion from the nearby Suez Canal Navigation Route and dewatering wells (Conjunctive use of groundwater) along the western sector of the study area. These two models could help in increasing the cultivation areas, improving the soil salinity and save up to 1.8 billion  $\text{m}^3/\text{year}$  (5 million  $\text{m}^3/\text{day}$ ) of the Nile water, which is lost by evaporation from the prevailed wetlands, water seepage and return flow from the surface water system, concerning an average direct evaporation rate of 5 ml/day prevailed in the study area. Design of drainage system depends on many factors, which are; maximum height of water table; soil texture and characteristics; drainage rate and depths of the restricting layer. The simplest equations based on the assumption of horizontal flow, which is valid only if the impermeable restricting layer is at small distance below the drain as in our case of study. Determinations of drain spacing and effective depths in the study area were done using Hooghoudt equation (Hooghoudt, 1940 and Schilfgaard, 1957) as follows:

$$v_a = 4Km (2D_e + m) / L^2$$

Where,  $v_a$  is drainage rate (function of irrigation rate),  $K$  is hydraulic conductivity (varies between 0.4-3.9),  $D_e$  is effective depth of restricting layer below drain center (1-3m),  $m$  is height of water table above drain centres midway between drains (0.5-2m) and  $L$  is the spacing distance between drains (variable according to the soil and hydraulic properties).

Water heads, average discharge, hydraulic conductivity, storage coefficient and thickness of aquifer at proposal area were simulated using the MODFLOW program (Mc Donald and Harbough, 1988). The calculation procedure was iterated several times, until a steady state flow has been obtained. The obtained results for the underground tile drain design indicated that, the estimated drainage spacing is varying between 111 m in case of using flood irrigation techniques (rate of irrigation is about 0.023 m/d) and 145 m for drip irrigation techniques (rate of irrigation is about 0.014 m/d (Bouwer, 1978) along the water logged

stretch, west of Bitter Lakes (Fig. 12). In case of existing an upward leakage factor from the underlying leaky confining layer of an order of 0.015m/d and an evaporation rate of an average value of 0.006m/d (Geriesh, 1995). This means that the average net recharge to the logged site is equal to 0.008 m/d. This dewatering model reduces water level along the cultivated lands from 1.5- 3 meters (Fig. 13). For quick removal of excess irrigated water, construction of more surface drains following the natural gradient is required. The surface drains need to be properly maintained and reconditioned from time to time. The existing drains should be cleared of the weeds and the sediments, which have reduced their carrying capacity and enhance their primary objective. Further all the surface drains should be linked to the field drains through link drains to dispose excess water; else there construction won't solve the purpose. It is recommended to reuse the logged water for expanding irrigation to the neighboring desert fringes to the eastern and southern sectors.

## CONCLUSION

Data integration and analysis indicate that the area is under threats by five types of geoenvironmental hazards which are; Waterlogging (water loss); soil salinization; water pollution; land subsidence; and land degradation. The wetland areas had increased from 930  $\text{km}^2$  in 1989 to 1044  $\text{km}^2$  in 2014. In addition the area covered by salt crust has increased from 360  $\text{km}^2$  in 1989 to 1356  $\text{km}^2$  in 2014. Urban land use and designed cultivated lands were also increased from 3620  $\text{km}^2$  in 1989 to 3760  $\text{km}^2$  in 2014. There are several factors controlling land cover changes including groundwater and sea level rise, land subsiding, inadequate drainage distribution and increasing of fish farming areas. Three main reasons of waterlogging are distinguished in the study area which are: (1) the development of a perched aquifer (duplex soil structure) over an extendable salty clay layer along the northern El-Tina Plain area; (2) the topographic relieve changes and inundation of several micro-depressional zones in the low lying areas along the northern sector and within the sand dune accumulations; (3) Seepage from surface water system

and its surrounding irrigation activities. Soil salinization is highly related to the waterlogging, soil composition, depth to perched layer and high evaporation rate that prevailed in the study area.

Waterlogging risk at the study area was confirmed and outlined using the aforementioned discussed remote sensing and hydrogeologic data from 1980 to 2014. The area witnessed a rapid agricultural development in the past three decades, and the environmental changes were very remarkable. Therefore, the present study gives some mitigation measures for the predicted hazards.

To remediate the problem, improving drainage density and reuse the logged water through pumping to the neighbouring desert fringes are recommended. The present study proposes solution models for improving drainage efficiency using dewatering underground drain approach which will help bringing down the high water level and coping with shortage of water by saving up to 1.8 billion m<sup>3</sup>/year (5 million m<sup>3</sup>/day) of the Nile water, which is lost by evaporation from the prevailed wetlands, water seepage and return flow from the surface water system.

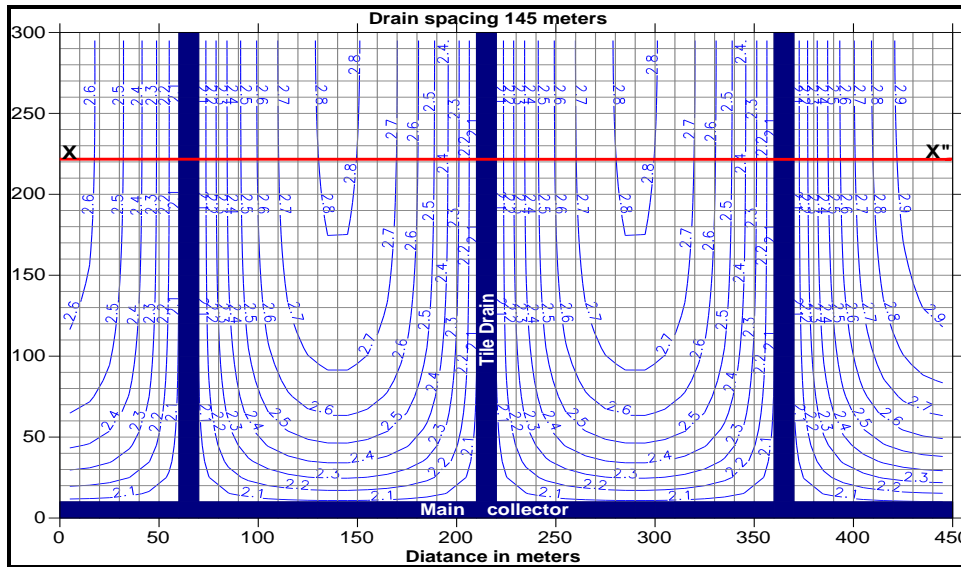


Figure (12): A case study of dewatering flow model of the proposed tile drain design along the logged water sites, west of Bitter lakes.

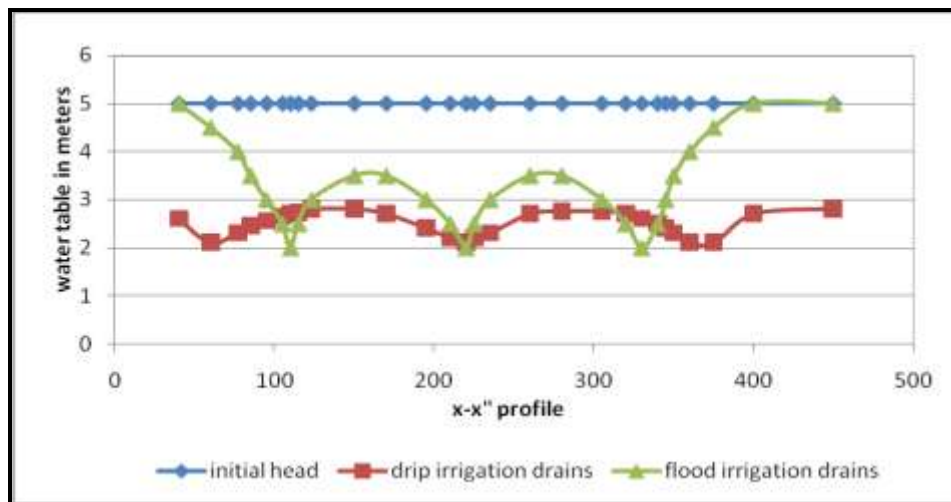


Figure (13): Cross section of the dewatering underground tile drains model along water logged areas, west of Bitter Lakes.

**REFERENCES**

APHA. 1971. Standard methods for the examination of water and waste water, 13th ed. Am. Public Health Assoc., Washington, D.C., 874 pp.  
 ARNOUS, M. O., AND D. R. GREEN. 2015. Monitoring and assessing waterlogging and salt-

affected areas in the Eastern Nile Delta region, Egypt, using remotely sensed multi-temporal data and GIS. J Coast Conserv, DOI 10.1007/s11852-015-0397-5.  
 AYERS, R. S. 1975. Quality of water for irrigation. Proc. Irri. Drain. Div., Specialty Conf., Am. Soc.

- Civ. Eng. August, 13-15, Logan, Utah, pp. 24-56.
- BOUWER, H. 1978. Groundwater Hydrology, 480 p. McGraw-Hill Series in Water Resources and Environmental Engineering. Library of Congress, Washington DC. USA. P. 294-299.
- EHCW. 1995. Egyptian Higher Committee of Water, Egyptian drinking water regulation standards according to the law 27/1978.
- EPA. 1975. US Environmental Protection Agency, National interim primary drinking water regulations, Part 141. Federal Register **40** (248): 59566-59588.
- FRIHY, O. E. 1992. Sea-level rise and shoreline retreat of the Nile delta promontories, Egypt. Natural Hazards **5**: 65-81.
- GERIESH, M. H. 1989. Hydrogeological investigations of West Ismailia area, Egypt. M.Sc. Thesis, Suez Canal University, Ismailia, Egypt.
- GERIESH, M. H. 1995. Hydrogeological and hydrogeochemical evaluation of groundwater resources at Suez Canal Province, Egypt. Ph.D. Thesis, Suez Canal University, Ismailia, Egypt.
- HOOGHOUTD, S. B. 1940. Bijdragen tot de kennis van eenige natuurkundige grootheden van de grond. Verslagen Landbouwk. Onderz.. **46** (14B): 515 - 707, Government Printing Office, The Hague, Netherlands.
- KLEMAS, V., AND A. M. ABDEL KADER. 1982. Remote sensing of coastal processes with emphasis on the Nile delta. In: Proceedings of the international symposium on remote sensing of environments, Cairo, 27p.
- MC-DONALD, M. G., AND A. HARBOUGH. 1988. A modular three-dimensional finite-difference groundwater flow model. US. Geol. Survey, open-file report, 83-875.
- SCHILFGAARDE, J. V. 1957. Approximate solutions to drainage flow problems. In: J.N.Luthin (Ed.), Drainage of agricultural lands, p.79-112. Agron. Monogr. 7. ASA, Madison, WI, USA.
- SHATA, A. AND I. F. EL FAYOMY 1970. Remarks on the hydrogeology of the Nile Delta. Proc. symp. Hydrogeology of Deltas, UNESCO v. II.
- ZAGHLOUL, Z. M., H. H. TAHA., O. A. HEGAB, AND F. M. EL-FAWAL. 1979. The Plio-Pliostocene Nile Delta subenvironments; Stratigraphic section and genetic class. Geol. Soc. Vol. 1x, Cairo.

## تأثيرات الأنشطة البشرية على النظام الهيدروجيولوجي لشرق دلتا النيل ، مصر

بسمه محمد حلمي منصور، أحمد السيد الرئيس، منى فؤاد قيصير  
قسم الجيولوجيا ، كلية العلوم ، جامعة قناة السويس، الإسماعيلية ، ٤١٥٢٢ ، مصر

### الملخص العربي

تساهم الأنشطة البشرية بالعديد من التهديدات الهيدروجيولوجية مثل غرق الأراضي وتملح التربة وتلوث المياه الجوفية بمنطقة شرق دلتا النيل. وقد استخدمت الصور الفضائية لإكتشاف التغيرات البيئية بالمنطقة خلال الثلاثة عقود الماضية. وبتكامل بيانات صور الأقمار الصناعية بإستخدام نظم المعلومات الجغرافية تم مراقبة وقياس المساحات السطحية للمناطق الزراعية والحضرية وبناء خرائط مخاطر غرق المياه وتملح التربة. وأظهرت النتائج أن المياه المفقودة بتأثير البحر من مناطق الغدق المائي ومن مناطق الري بالغمر بلغت نسبتها حوالي ٣٠% من إجمالي المياه المفقودة من المنطقة. كما أن مساحة الأراضي الغارقة بمياه الغدق المائي قد إزدادت من ٢كم<sup>2</sup> عام ١٩٨٤ إلى ١٨٠كم<sup>2</sup> عام ٢٠١٤ على طول سهل الطينة الذي يمثل أكثر المناطق عرضة لهذا التهديد. كما أشارت النتائج إلى أن إجمالي فقد المياه بالبحر المباشر وصل إلى ٢٣.٦ مليار متر<sup>3</sup>/سنة. وأوضحت النتائج أن بعد حفر ترعة السلام قلت كميات المياه المتسربة إلى بحيرة المنزلة مما أدى إلى تناقص مساحة البحيرة بحوالي ٤٥% من إجمالي مساحتها قبل حفر الترعة. كما أنه تدهورت جودة مياه البحيرة بصورة شديدة نتيجة لإلقاء مياه الصرف الصحي والزراعي فيها.